Published in final edited form as:
Angew Chem Int Ed Engl. 2011 July 4; 50(28): 6258–6263. doi:10.1002/anie.201102459.

Synthesis and In Vivo Fate of Zwitterionic Near-Infrared Fluorophores**

Hak Soo Choi, **Khaled Nasr**, **Sergey Alyabyev**, **Dina Feith**, **Jeong Heon Lee**, **Soon Hee Kim**, **Yoshitomo Ashitate**, **Hoon Hyun**, **Gabor Patonay**, **Lucjan Strekowski**, **Maged Henary**[*], and **John V. Frangioni**[*]

H.S. Choi, Ph.D., K. Nasr, Ph.D., D. Feith, M.S., J.H. Lee, B.S., S.H. Kim, Ph.D., Y. Ashitate, M.D., H. Hyun, Ph.D., J.V. Frangioni, M.D., Ph.D. Division of Hematology/Oncology, Department of Medicine and Department of Radiology, Beth Israel Deaconess Medical Center, 330 Brookline Avenue, SLB-05, Boston, MA, 02215, USA. S. Alyabyev, Ph.D., G. Patonay, Ph.D., L. Strekowski, Ph.D., M. Henary, Ph.D., Department of Chemistry, Georgia State University, Atlanta, GA 30303, USA. S.H. Kim, Ph.D., WCU Department of BIN Fusion Technology, Chonbuk National University, Jeonju 561-756, South Korea

Keywords

Near-Infrared Fluorophores; Fluorescence Optical Imaging; Image-Guided Surgery; Biodistribution; Clearance

A longstanding problem in the field of image-guided surgery is the development of ideal near-infrared (NIR) fluorophores. The heptamethine NIR fluorophore indocyanine green (ICG) has been used extensively for image-guided surgery because of clinical availability and safety.[1-3] However, ICG is far from ideal because it exhibits high uptake in the liver, contaminates the gastrointestinal (GI) tract, provides moderate optical properties,[4] is unstable in aqueous media,[3,5] and is unable to conjugate covalently to targeting ligands.[2] Although several classes of novel molecules have been described,[6-13] none to date exhibit simultaneous low background binding, bifunctionality, excellent optical properties, low protein binding, and high serum stability. Although it is intuitive that physicochemical properties, i.e., positive/negative charge density, hydrophilicity/lipophilicity, and charge distribution, will impact *in vivo* performance, chemical structures that exhibit ideal characteristics have not yet been defined.

Previously, our group showed that rigid spherical nanoparticles, such as quantum dots, with a hydrodynamic diameter (HD) ≤ 5.5 nm could be rapidly cleared by the kidneys, and exhibit low background binding to normal tissues and organs, but only when the surface charge was neutral, geometrically balanced, and polyionic (referred to herein as zwitterionic for simplicity).[14-19] In this study, we explored the hypothesis that NIR fluorescent small molecules would exhibit improved *in vitro* and *in vivo* performance if synthesized with

**This study was supported by the following grants from the National Institutes of Health: NCI BRP grant #R01-CA-115296 (JVF), NIBIB grant #R01-EB-010022 (JVF and HSC) and NIBIB grant #R01-EB-011523 (HSC and JVF). We thank Lindsey Gendall and Lorissa A. Moffitt for editing, and Linda Keys and Eugenia Trabucchi for administrative assistance. All FLARE™ technology is owned by Beth Israel Deaconess Medical Center, a teaching hospital of Harvard Medical School. As inventor, Dr. Frangioni may someday receive royalties if products are commercialized. Dr. Frangioni is the founder and unpaid director of The FLARE™ Foundation, a nonprofit organization focused on promoting the dissemination of medical imaging technology for research and clinical use.

[*] Fax: (+1) 617-667-0981, jfrangio@bidmc.harvard.edu Fax: (+1) 404-413-5505, chemmh@langate.gsu.edu.

zwitterionic charges that are evenly spaced over the molecule to shield the underlying hydrophobicity of the relatively large heptamethine core.

We describe 2 complementary molecules, termed ZW800±*i* where ±*i* is the charge of the conjugated targeting ligand that will render the final molecule with a net charge of zero (i.e., zwitterionic). ZW800-1 has a net charge = 0 prior to targeting ligand conjugation, and a net charge = 0 after conjugation to a targeting ligand having a net charge of -1 (that is, a targeting ligand with a net charge of 0 prior to conjugation). ZW800-3a has a net charge = +2 prior to conjugation, and a net charge = 0 after conjugation to a targeting ligand having a net charge of -3 (that is, a targeting ligand with a net charge of -2 prior to conjugation). ZW800-1 and ZW800-3a were engineered for high hydrophilicity, with logD (distribution coefficient) at pH 7.4 of -3.56 and -6.95, respectively. Importantly, these molecules have also been engineered with sulfonate groups to impart negative charge and quaternary ammonium cations (quats) to impart positive charge because preliminary results showed that the weaker, more common natural analogs (carboxylic acids and primary amines, respectively) did not exhibit desired properties.

As depicted in **Figure 1a**, chloro-substituted NIR fluorophores **8** and **9** were synthesized by employing quats and/or sulfonates (**5** or **6**) on the indocyanine backbone. Vilsmeier-Haack reagent **7** was synthesized and used for the condensation reaction with prepared intermediate indolium salts in anhydrous sodium acetate. Finally, to permit subsequent conjugation of targeting ligands and biomolecules, a bifunctional phenoxypropionic acid linkage was introduced on the *meso*-chlorine atom. Using microwave synthesis, we were able to achieve an extremely high conversion ratio (> 98%) and yield (> 85%) of the final reaction (**Table S1**). The crude product was washed with ether 3 times and precipitated with methanol and ether (20 mL, 1:4) to yield the final compounds **10** (ZW800-1) and **11** (ZW800-3a) as a dark green solid. Chemical purity of ZW800-1 and ZW800-3a was 97.1% and 98.7%, respectively (**Figure 1b**). ^{1}H NMR, ^{13}C NMR, and ES-TOF MS were consistent with the proposed structures (**Figures S1-S2**). Due to the polar and hygroscopic nature of the final compounds, both ZW800-1 and ZW800-3a included 4 extra water molecules, analyzed by CHN elemental analysis. See **Supporting Information** for detailed chemical syntheses and analyses.

The hypothesis guiding our work was that zwitterionic small molecules might recapitulate the results seen previously with nanoparticles, namely lower *in vivo* background. To test this hypothesis, we analyzed a series of heptamethine indocyanine NIR fluorophores that systematically varied in net charge as follows: -4 (CW800), -2 (RS800), -1 (ICG), 0 (ZW800-1), and +2 (ZW800-3a). The chemical structures and energy-minimized 3-D structures of these NIR fluorophores are shown in **Figure 2a**. A note should be made of the significantly different distributions of charge and hydrophobicity over the surface of each molecule. The physicochemical and optical properties of these fluorophores are detailed in **Table 1**, **Figures 2b**, **S3-S4**. Although net charge and logD at pH 7.4 varied widely, most optical parameters were similar and all compounds were stable (> 94%) in warm serum for up to 4 h.

Serum protein binding was measured by gel filtration chromatography (GFC) after incubating in 100% serum (**Figure S5**). ICG, which is known to bind serum proteins such as α_1-lipoprotein, γ-globulin, and serum albumin,[4,20] showed a significant HD shift after 4 h incubation in FBS due to its hydrophobic character (logD = 7.88) and net negative charge (+1/-2, net charge = -1). However, ZW800-1, with high hydrophilicity (logD = -3.56) and balanced, alternating charge (+3/-3, net charge = 0) distributed evenly over its surface, did not adsorb to serum proteins. Although its logD value at pH 7.4 is extremely low (-6.95),

ZW800-3a showed low levels of protein adsorption when exposed to 100% serum, likely due to its unbalanced charge distribution (+3/-1, net charge = +2).

To investigate the effect of chemical structure and net charge on *in vivo* biodistribution and clearance, the NIR fluorophore series was injected intravenously into mice and rats. Using the Fluorescence-Assisted Resection and Exploration (FLARE™) intraoperative image-guided surgery system,[21,22] we measured the behavior of injected fluorophores in real time over 4 h. As shown in **Figure 3a**, the β-phase blood half-life ($t_{1/2\beta}$) of CW800 (-4), RS800 (-2), ICG (-1), ZW800-1 (0), and ZW800-3a (+2) in CD-1 mice was 18.5, 11.2, 3.6, 15.1, and 28.1 min, respectively. All half-life values were statistically different from each other by ANOVA. Elimination of NIR fluorophores from the body via renal clearance also varied markedly (**Table 2**), with ICG being undetectable in urine (due to liver uptake and subsequent biliary clearance) and ZW800-1 being mostly renally cleared. The fraction of the injected dose that was eliminated from the body into urine by 4 h postinjection in mice was 44.0 ± 4.6 %ID, 15.5 ± 1.2 %ID, 2.2 ± 0.9 %ID, 86.0 ± 15.4 %ID, and 23.2 ± 11.4 %ID, respectively for CW800 (-4), RS800 (-2), ICG (-1), ZW800-1 (0), and ZW800-3a (+2) (see also **Figures S6-S8**). In fact, after only 1 h post-injection, 51.3 ± 9.7 %ID of ZW800-1 was found in urine.

Uptake of NIR fluorophores in organs and tissues of mice and rats also varied markedly. As shown in **Figure 3b** (see also **Figures S6-S8** and **Videos S1-S3**), all anionic and cationic NIR fluorophores exhibited high non-specific uptake in a variety of organs, with anionic NIR fluorophores exhibiting significant excretion into bile, resulting in high NIR fluorescent signal throughout the GI tract. For example, at 4 h postinjection, uptake values for CW800 (-4) were intestine (28.5 ± 7.0 %ID/g), liver (11.4 ± 0.8 %ID/g), and kidneys (7.3 ± 1.3 %ID/g). For ICG (-1), uptake values were intestine (62.0 ± 6.6 %ID/g), liver (27.1 ± 0.5 %ID/g), and kidneys (5.9 ± 1.0 %ID/g), which were also caused by the extremely high hydrophobicity/lipophilicity (logD at pH 7.4 = 7.88). Two positive charges of ZW800-3a (+2) resulted in unfavorable biodistribution, mostly found in the liver (40.6 ± 2.6 %ID/g), intestine (11.5 ± 3.4 %ID/g), and kidneys (9.0 ± 1.1 %ID/g). On the contrary, ZW800-1 was exclusively cleared by the kidneys, with no appreciable non-specific background signal in any tissues and organs and only 12.4 ± 3.4 %ID remaining in the carcass at 4 h post-injection, mostly in the kidneys (9.8 ± 2.2 %ID/g) and only negligible amounts in the liver (0.9 ± 0.1 %ID/g) and intestine (0.7 ± 0.4 %ID/g). Similar results were observed in rats, but excretion rates were slightly slower than those in mice (**Table 2**). It should be emphasized that no single value, such as logD or net charge, is predictive of *in vivo* fate. Optimal *in vivo* behavior appears to be mediated by alternating and balanced charge, distributed over the entire surface of the molecule, which completely shields underlying hydrophobicity.

The most common strategy to engineer targeted NIR fluorescent contrast agents is to employ "modular" chemistry,[23-25] which covalently combines a NIR fluorophore and a high-affinity, small molecule targeting ligand. However, commercially available NIR fluorophores are typically hydrophobic and/or di-/tetra-sulfonated. One of the key results of our study is that purely anionic or cationic NIR fluorophores exhibit significant non-specific uptake in normal tissues and organs, although their logD at 7.4 is extremely low (i.e., hydrophilic). For molecules that have a high "hydrophobic moment" like ICG, liver uptake was significant and rapid, thus reducing blood concentration, but increasing NIR fluorescence of the liver, bile, and GI tract.[26] This contaminates the liver and/or lower GI tract with high signal and precludes many important image-guided surgeries of the abdomen. The blood half-life of ICG was only 2 to 5 minutes because of rapid liver uptake. RS800 had a lower hydrophobic moment, but still had exposed aromatic groups that were recognized by the liver and resulted in rapid excretion into bile (short transit time through the liver). However, it also had enough charge to keep it in the bloodstream long enough to undergo ≈

20% renal filtration. For highly anionic CW800, the hydrophobic moment was compensated by the charge (more hydrophilic), resulting in ≈ 55% renal filtration,[27] but also significant liver clearance,[28] GI tract contamination, and non-specific uptake in normal tissues and organs. The high cationic charge of ZW800-3a caused the molecule to exhibit high non-specific uptake in almost every tissue and organ in the body, resulting in only ≈ 20% renal excretion. Only a true zwitterionic molecule, such as ZW800-1, with charge balanced over the entire surface and hydrophobicity well-shielded by this charge, does not exhibit protein binding, non-specific tissue/organ uptake, or liver clearance. Although the precise mechanism for this observation is not yet known, zwitterionic molecules likely minimize interaction with serum proteins via charge shielding,[29] and minimize penetration of cellular membranes via extreme polarity.[30,31]

Because our efforts focused on lowering background, it would have been counter-productive if this were achieved at the expense of signal. This is a major problem, for example, when utilizing two-photon, upconversion strategies for NIR fluorescence. Fortunately, we demonstrate that the optical properties of zwitterionic NIR fluorophores are excellent. In fact, the product of ZW800-1's extinction coefficient and quantum yield in serum are over 3-fold higher than that of the FDA-approved NIR fluorophore ICG (**Table 1**). In addition, the 800 nm zwitterionic heptamethine indocyanine NIR fluorophore ZW800-1 has remarkable *in vivo* properties, including no serum protein binding, rapid renal clearance, and ultralow non-specific tissue uptake (i.e., background). ZW800-1 also provides a single carboxylic acid for covalent conjugation to targeting ligands through a stable amide bond. Because of these features, ZW800-1 has been selected by the US National Cancer Institute's Experimental Therapeutics (NExT) Program as a first-in-class molecule for rapid translation into human clinical studies.

A key unanswered question in the present study is whether a targeted NIR fluorophore made zwitterionic by choosing the proper ZW800±*i* fluorophore for conjugation requires intermingled positive and negative charges over the entire surface of the final molecule (similar to unconjugated ZW800-1), or whether a dipole-like zwitterionic structure is adequate for improved *in vivo* performance. Ongoing studies are also focused on the engineering of a family of 700 nm zwitterionic NIR fluorophores to complement those we now have at 800 nm. When used with the 2 NIR channel capabilities of the FLARE™ imaging system, it should then be possible to simultaneously image 2 independent targeted NIR fluorophores during surgery. This is especially important in cancer surgery when resection of the tumor (i.e., using 1 NIR channel) needs to be performed while avoiding critical structures such as vessels and nerves (i.e., using the second NIR channel).

Experimental Section

Synthesis of ZW800-1 (10) and ZW800-3a (11)

As depicted in **Figure 1a**, starting materials **1-4** were used to prepare the 800 nm emitting, zwitterionic heptamethine indocyanine fluorophores **10** (ZW800-1) and **11** (ZW800-3a). All products **5-11** were obtained in reasonably high purity as indicated by TLC analyses using C18 adsorbents and high-resolution ^{1}H and ^{13}C nuclear magnetic resonance (NMR) spectra. Chemical purity was measured by using high-performance liquid chromatography (HPLC) combined with simultaneous evaporative light scatter detection (ELSD), absorbance (photodiode array), fluorescence, and electrospray time-of-flight (ES-TOF) mass spectrometry (MS). Compounds were also analyzed by matrix-assisted laser desorption/ ionization (MALDI) TOF MS and CHN elemental analysis. See **Supporting Information** for detailed chemical syntheses and analyses.

Optical and Physicochemical Property Analyses

Commercially available NIR fluorophores included IRDye™ 800-CW (CW800; Li-Cor, Lincoln, NE), IRDye™ 800-RS (RS800; Li-Cor), and indocyanine green (ICG; Akorn, Decatur, IL). When only an NHS ester was available, the corresponding carboxylic acid (CA) was formed by incubation at high concentration in 50 mM borate buffer, pH 9.0 for 3 h followed by dilution into the desired buffer. All optical measurements were performed at 37°C in phosphate-buffered saline (PBS), pH 7.4 or 100% fetal bovine serum (FBS) buffered with 50 mM HEPES, pH 7.4. For fluorescence quantum yield (Φ) measurements, ICG in dimethyl sulfoxide (Φ = 13%) was used as a calibration standard under conditions of matched absorbance at 770 nm.[14-19] For *in vitro* optical property measurements, online fiberoptic HR2000 absorbance (200-1100 nm) and USB2000FL fluorescence (350-1000 nm) spectrometers (Ocean Optics, Dunedin, FL) were used. NIR excitation was provided by a 770 nm NIR laser diode light source (Electro Optical Components, Santa Rosa, CA) set to 8 mW and coupled through a 300-μm core diameter, NA 0.22 fiber (Fiberguide Industries, Stirling, NJ). *In silico* calculations of the partition coefficient (logD) and surface molecular charge and hydrophobicity were calculated using MarvinSketch 5.2.1 (ChemAxon, Budapest, Hungary).

In Vivo Biodistribution and Clearance

Animals were housed in an AAALAC-certified facility and were studied under the supervision of an approved institutional protocol. CD-1 male mice weighing 25 to 30 g and Sprague-Dawley (SD) male rats weighing 250 to 300 g were purchased from Charles River Laboratories (Wilmington, MA). 40 pmol/g of NIR fluorophores in saline were administered intravenously, and animals were imaged with the FLARE™ real-time intraoperative imaging system as described in detail previously.[21] For fluorescence excitation, 14 mW/cm^2 of 745 to 779 nm-filtered light was used, and for emission, light was filtered using a 800 to 848 nm bandpass filter. For each experiment, camera exposure time and image normalization was held constant. Color video images were collected on a separate channel using custom-designed optics and software. To quantify the blood clearance rate and urinary excretion, intermittent sampling from the tail vein was performed over 4 h. Approximately 20 L of blood and urine were collected at the following time points using glass capillary tubes: 0, 1, 2, 5, 10, 15, 30, 60, 90, 120, 180, and 240 min. The FLARE™ imaging system measured the fluorescence intensity of each sample, and the concentration was calculated based on CBR (defined below) using a standard curve for each fluorophore. To measure total body excretion in mice, animals were sacrificed at 30, 60, 90, 120, 180, and 240 min, and major tissues and organs were resected, lyophilized, weighed, and re-dissolved in tissue lysate buffer. The tissue containing solutions were homogenized using a bullet blender (Next Advance, Averill Park, NY). Using capillary tubes, the amount of NIR fluorophore in each organ/tissue was quantified by measuring fluorescent intensity (CBR), which was converted to concentration (%ID/g) or amount (%ID) based on organ/tissue weight.

Quantitative Analysis

At each time point, the fluorescence (FL) and background (BG) intensity of a region of interest (ROI) over each organ/tissue was quantified using custom FLARE™ software. The contrast-to-background ratio (CBR) was calculated as CBR = (FL–BG)/BG. At least 3 animals were analyzed at each time point. Statistical analysis was carried out using the unpaired Student's *t* test or one-way analysis of variance (ANOVA). Results were presented as mean ± S.D. and curve fitting was performed using Prism version 4.0a software (GraphPad, San Diego, CA).

Supplementary Material

Refer to Web version on PubMed Central for supplementary material.

References

1. Frangioni JV. Curr Opin Chem Biol. 2003; 7:626–634. [PubMed: 14580568]
2. Kobayashi H, Ogawa M, Alford R, Choyke PL, Urano Y. Chem Rev. 2009
3. Achilefu S. Angew Chem Int Ed Engl. 2010; 49:9816–9818. [PubMed: 21089086]
4. Ohnishi S, Lomnes SJ, Laurence RG, Gogbashian A, Mariani G, Frangioni JV. Mol Imaging. 2005; 4:172–181. [PubMed: 16194449]
5. Lee H, Mason JC, Achilefu S. J Org Chem. 2006; 71:7862–7865. [PubMed: 16995699]
6. Strekowski L, Lipowska M, Patonay G. J Org Chem. 1992; 57:4578–4580.
7. Patonay G, Salon J, Sowell J, Strekowski L. Molecules. 2004; 9:40–49. [PubMed: 18007410]
8. Zhang Z, Liang K, Bloch S, Berezin M, Achilefu S. Bioconjug Chem. 2005; 16:1232–1239. [PubMed: 16173803]
9. Kiyose K, Kojima H, Urano Y, Nagano T. J Am Chem Soc. 2006; 128:6548–6549. [PubMed: 16704241]
10. Kobayashi H, Koyama Y, Barrett T, Hama Y, Regino CA, Shin IS, Jang BS, Le N, Paik CH, Choyke PL, Urano Y. ACS Nano. 2007; 1:258–264. [PubMed: 19079788]
11. Chen K, Xie J, Chen X. Mol Imaging. 2009; 8:65–73. [PubMed: 19397852]
12. Lee S, Ryu JH, Park K, Lee A, Lee SY, Youn IC, Ahn CH, Yoon SM, Myung SJ, Moon DH, Chen X, Choi K, Kwon IC, Kim K. Nano Lett. 2009; 9:4412–4416. [PubMed: 19842672]
13. Hilderbrand SA, Weissleder R. Curr Opin Chem Biol. 2010; 14:71–79. [PubMed: 19879798]
14. Choi HS, Liu W, Misra P, Tanaka E, Zimmer JP, Itty Ipe B, Bawendi MG, Frangioni JV. Nat Biotechnol. 2007; 25:1165–1170. [PubMed: 17891134]
15. Liu W, Choi HS, Zimmer JP, Tanaka E, Frangioni JV, Bawendi M. J Am Chem Soc. 2007; 129:14530–14531. [PubMed: 17983223]
16. Choi HS, Ipe BI, Misra P, Lee JH, Bawendi MG, Frangioni JV. Nano Lett. 2009; 9:2354–2359. [PubMed: 19422261]
17. Choi HS, Liu W, Liu F, Nasr K, Misra P, Bawendi MG, Frangioni JV. Nat Nanotechnol. 2010; 5:42–47. [PubMed: 19893516]
18. Choi HS, Ashitate Y, Lee JH, Kim SH, Matsui A, Insin N, Bawendi MG, Semmler-Behnke M, Frangioni JV, Tsuda A. Nat Biotechnol. 2010; 28:1300–1303. [PubMed: 21057497]
19. Choi HS, Frangioni JV. Mol Imaging. 2010; 9:291–310. [PubMed: 21084027]
20. Williams RJ, Lipowska M, Patonay G, Strekowski L. Anal Chem. 1993; 65:601–605. [PubMed: 8452246]
21. Troyan SL, Kianzad V, Gibbs-Strauss SL, Gioux S, Matsui A, Oketokoun R, Ngo L, Khamene A, Azar F, Frangioni JV. Ann Surg Oncol. 2009; 16:2943–2952. [PubMed: 19582506]
22. Gioux S, Choi HS, Frangioni JV. Mol Imaging. 2010; 9:237–255. [PubMed: 20868625]
23. Humblet V, Misra P, Frangioni JV. Contrast Media Mol Imaging. 2006; 1:196–211. [PubMed: 17193697]
24. Ye Y, Bloch S, Xu B, Achilefu S. Bioconjug Chem. 2008; 19:225–234. [PubMed: 18038965]
25. Qian H, Gu Y, Wang M, Achilefu S. J Fluoresc. 2009; 19:277–284. [PubMed: 18758925]
26. Matsui A, Tanaka E, Choi HS, Winer JH, Kianzad V, Gioux S, Laurence RG, Frangioni JV. Surgery. 2010; 148:87–95. [PubMed: 20117813]
27. Tanaka E, Ohnishi S, Laurence RG, Choi HS, Humblet V, Frangioni JV. J Urol. 2007; 178:2197–2202. [PubMed: 17870110]
28. Tanaka E, Choi HS, Humblet V, Ohnishi S, Laurence RG, Frangioni JV. Surgery. 2008; 144:39–48. [PubMed: 18571583]
29. Colton IJ, Carbeck JD, Rao J, Whitesides GM. Electrophoresis. 1998; 19:367–382. [PubMed: 9551788]

30. Bourre L, Giuntini F, Eggleston IM, Wilson M, MacRobert AJ. Br J Cancer. 2009; 100:723–731. [PubMed: 19240715]

31. Zwaal RF, Comfurius P, van Deenen LL. Nature. 1977; 268:358–360. [PubMed: 887167]

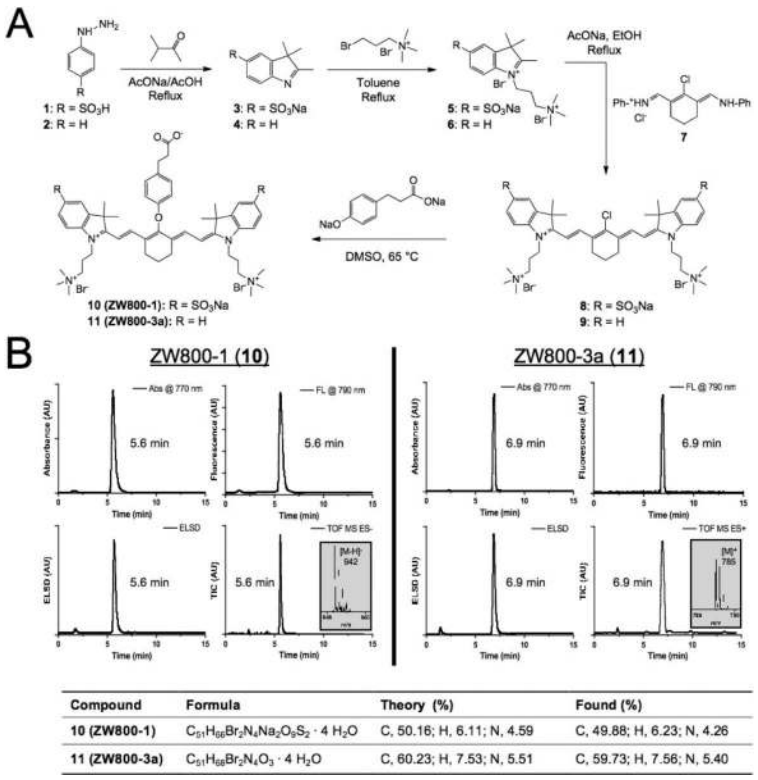

Compound	Formula	Theory (%)	Found (%)
10 (ZW800-1)	$C_{61}H_{66}Br_2N_4Na_2O_9S_2 \cdot 4\ H_2O$	C, 50.16; H, 6.11; N, 4.59	C, 49.88; H, 6.23; N, 4.26
11 (ZW800-3a)	$C_{61}H_{66}Br_2N_4O_3 \cdot 4\ H_2O$	C, 60.23; H, 7.53; N, 5.51	C, 59.73; H, 7.56; N, 5.40

Figure 1.

Synthesis and characterization of 800 nm zwitterionic heptamethine indocyanine NIR fluorophores (ZW dyes). **A**) Synthetic scheme for zwitterionic heptamethine indocyanine NIR fluorophores. **B**) LC-MS and elemental analysis: absorbance at 770 nm (top left), fluorescence (λ_{ex} = 770 nm and λ_{em} = 790 nm; top right), ELSD (bottom left), and total ion chromatogram (TIC; bottom right). Insert = ESI-TOF mass spectrum (-) of 5.6 min peak for ZW800-1 and 6.9 min peak for ZW800-3a.

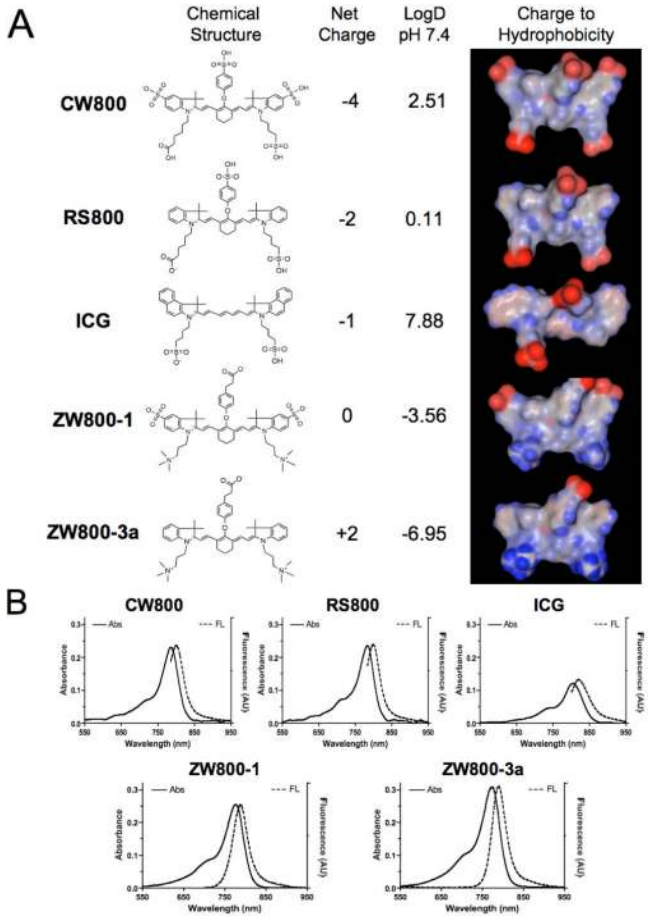

Figure 2.

Physicochemical and optical properties of NIR fluorophores having systematically varying net charge. **A**) All molecules shown are bifunctional, permitting conjugation via their single carboxylic acid group, except ICG. Red = negative charge; Blue = positive charge; Gray = hydrophobicity. **B**) Absorbance and fluorescence emission spectra of 1 μM each fluorophore in 100% FBS supplemented with 50 mM HEPES, pH 7.4.

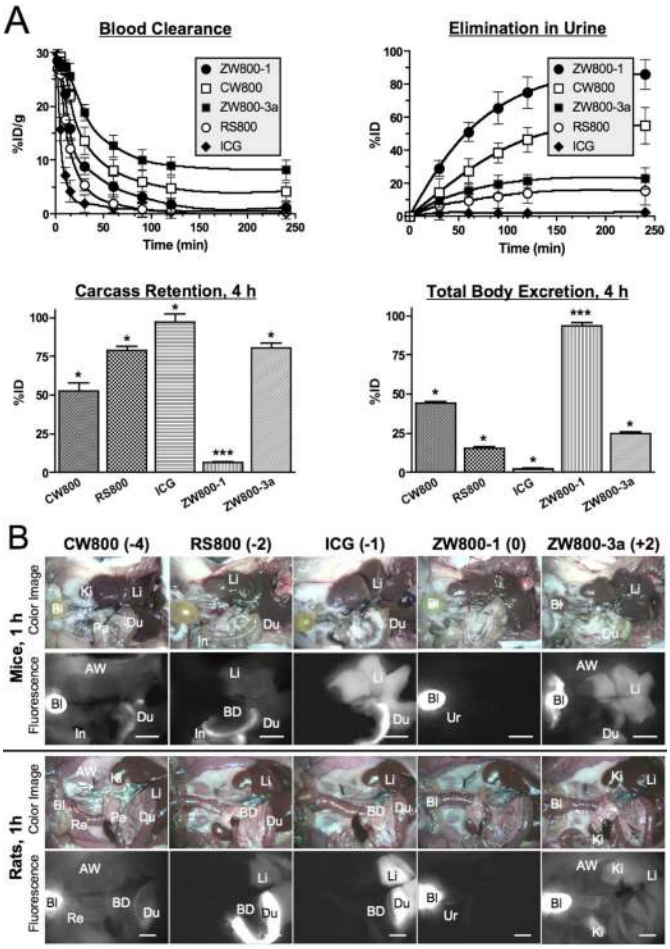

Figure 3.

Biodistribution and clearance of NIR fluorophores. **A**) Blood concentration (%ID/g), elimination in urine (%ID), carcass retention (%ID), and total body clearance (%ID) in CD-1 mice. Each data point is the mean ± S.D. from N = 5 animals. **P* < 0.01 and ****P* < 0.001 for pair wise comparisons of half-life using ANOVA. **B**) 40 pmol/g of NIR fluorophores were injected intravenously into CD-1 mice (top two panels) and SD rats (bottom two panels), 1 h prior to imaging. Shown are color and 800 nm NIR fluorescence images of surgically exposed organs/tissues. Abbreviations used are: AW, abdominal wall; Bl, bladder; BD, bile duct; Du, duodenum; In, intestine; Ki, kidneys; Li, liver; Lu, lungs; Pa, pancreas; Re, rectum, Sk, skin; and Ur, ureter. Scale bars = 1 cm.

Table 1

Comparison of chemical and optical properties of variously charged NIR fluorophores in 100% FBS.

Property	CW800	RS800	ICG	ZW800-1	ZW800-3a
MW (Da)	1091	887	775	1149	945
Net Charge	-4	-2	-1	0	+2
LogD at pH 7.4	2.51	0.11	7.88	-3.56	-6.95
ε ($M^{-1}cm^{-1}$)	237,000	240,000	121,000	249,000	309,000
λ_{exc} (nm)	786	784	807	772	774
λ_{em} (nm)	800	800	822	788	790
Stokes Shift (nm)	14	16	15	16	16
Φ (%)	14.2	16.9	9.3	15.1	16.1
Decomposition (%)	4.0	4.4	5.9	5.5	3.8

CW800 = IRDye™800-CW carboxylic acid; ICG = indocyanine green; RS800 = IRDye™800-RS carboxylic acid; ZW = zwitterionic.

Angew Chem Int Ed Engl. Author manuscript; available in PMC 2012 July 4.

Table 2

In vivo organ/tissue distribution of variously charged NIR fluorophores 4 h postinjection into mice (N = 5) and rats (N = 5).

Fluorophore	Species	Ki	Sk/Mu	He/Lu	Sp	Li	In	Re	Bl	Carcass	Eliminated
CW800	Mouse	+	+	–	–	–	+++	++	+++	52.4 ± 9.6 %ID	44.0 ± 4.6 %ID
	Rat	++	+	–	–	+	+++	+	+++	N.D.	N.D.
RS800	Mouse	+	–	–	–	–	++	+++	++	79.0 ± 4.1 %ID	15.5 ± 1.2 %ID
	Rat	+	–	–	–	–	+++	++	–	N.D.	N.D.
ICG	Mouse	–	–	–	–	++	+++	+	–	97.1 ± 9.4 %ID	2.2 ± 0.9 %ID
	Rat	–	–	–	–	++	+++	+	–	N.D.	N.D.
ZW800-1	Mouse	–	–	–	–	–	–	–	+++	12.4 ± 3.4 %ID	86.0 ± 15.4 %ID
	Rat	+	–	–	–	–	–	–	+++	14.8 ± 6.5 %ID	83.4 ± 15.9 %ID
ZW800-3a	Mouse	+	+	–	–	++	+++	+	+++	68.6 ± 8.6 %ID	23.2 ± 11.4 %ID
	Rat	++	++	+	+	+++	++	–	+++	68.3 ± 15.7 %ID	28.7 ± 16.3 %ID

Abbreviations used are: Bl, bladder; He, heart; In, intestine; Ki, kidneys; Li, liver; Lu, lungs; Mu, muscle; Re, rectum; Sk, skin; Sp, spleen; and N.D., not done. All mouse values were measured directly. Shown for each measurement is mean ± S.D. The CBR of each organ/tissue relative to the abdominal wall was quantified and labeled as –, 0 to 1; +, 1 to 2; ++, 2 to 5; and +++, > 5.